Journal of Applied Sciences

ISSN 1812-5654

science alert

ANSInet
an open access publisher
http://ansinet.com

Journal of Applied Sciences 13 (19): 4046-4051, 2013
ISSN 1812-5654 / DOI: 10.3923/jas.2013.4046.4051

Influence of Crack Size on the Propagation Trend of Multiple Rail Surface Cracks under Rolling Contact Fatigue

[1]Liu Yuan and [2]Chao Mi
[1]College of Logistics Engineering, Shanghai Maritime University, 201306, China
[2]Container Supply Chain Technology Engineering Research Center, Shanghai Maritime University, 201306, China

Abstract: With the existence of a new rail crack near the old one, the load distribution would be modified at the rail surface and when the new crack was of different sizes, it would affect the propagation trend of the old crack to different extent. In this study, simulations of multiple cracks growth in rail under Rolling Contact Fatigue (RCF) were presented based on a 3D finite element model. More specifically, the focus was on the calculation of the stress intensity factors at the crack tip fronts of short surface cracks. A fatigue crack propagation model was expressed in terms of stress intensity factor and the material characteristic of the rail to estimate the crack propagation direction and propagation rate. The results showed that with the increase of the new crack size, the propagation rate of the old crack would be decreased both at its surface and at certain depth and the propagation direction of the old crack would bend to the new crack at the rail surface which might cause the old crack to join the new one into a bigger crack and result in a higher propagation rate.

Key words: Stress intensity factor, propagation direction, propagation rate, RCF, multiple rail surface cracks

INTRODUCTION

Rail defects like tongue lipping, head checks, squats, pitting and spalling (Lewis and Olsson, 2009) are quite common in today's rails. They can be a huge threat to the safety of the tracks and cause high cost in rail maintenance and operation. They are usually the results of repeated wheel-rail rolling contacts and mainly governed by factors including the magnitude of the traction forces, the axle load and as well as lubrication conditions and the environment the residual stress field in the rail (Fletcher *et al*., 2009; Cookson and Mutton, 2011; Makino *et al*., 2012).

Rolling contact analyses are studied based on semi-analytical methods (Hearle and Jonson, 1987) and Finite Element (FE) methods (Jiang *et al*., 2002). Crack growth under RCF with Linear Elastic Fracture Mechanics (LEFM) approach are of great concern in rail life study (Seo *et al*., 2011; Brouzoulis and Ekh, 2012). There have been a number of investigations that focused on determining Stress Intensity Factors (SIF) for cracks subjected to RCF (Keer *et al*., 1982; Benuzzi *et al*., 2003) which could be a very clear index to show the rail crack growth behavior. In recent studies, the influence of wear, inelastic material behavior, fluid pressurization, etc., are taken into account during the propagation of rail cracks (Canadinc *et al*., 2008; Donzella *et al*., 2005; Ringsberg, 2005; Dubourg and Lamacq, 2002; Fajdiga *et al*., 2007).

The state of the art concerning modeling of different surface cracks is mainly limited to a single rail crack. However, the rail defects are usually not single in existence, like head checks (Muster *et al*., 1996; Ringsberg, 2005). Under the act of rolling contact loading between rail and wheel, the propagation of the neighboring rail cracks will affect each other and may join together to result in either spalling or a new crack propagating downward and cause final rail fracture.

The aim of the current study is an attempt to study the propagation behavior of the neighboring cracks at the rail surface, especially the influence of the crack size. Owing to this, a 3D crack propagation FE model with two surface cracks is established in ABAQUS with the profiles of UIC60 rail and S1002 wheel. A model to predict the propagation rate of the crack is also established in terms of the SIF at crack tips and the material characteristics. Results like crack propagation direction and propagation rate from varying crack sizes are presented and quantatively compared to the condition with only single rail crack.

MATERIALS AND METHODS

Theoretical models: Crack propagation criteria and propagation direction under RCF.

Corresponding Author: Chao Mi, College of Logistics Engineering, Shanghai Maritime University, 201306, China

With LEFM approach, under the act of external loads, Stress Intensity Factor (SIF) in three modes K_I, K_{II} and K_{III} can be used as the index to indicate the stress intensity at the crack tips.

At present, there are lots of crack propagation criteria, mainly based on the calculation of K_I, K_{II} and K_{III} at the crack tips and the most commonly used criterion is put forward by Erdogan and Sih (1963). Based on their research, Kaneta *et al.* (1986) further worked on the propagation criterion and prediction of crack propagation direction of Mode I (open mode) crack and Mode II (shear mode) crack. Their calculation was carried with polar coordinates (r, θ -D-Dd-La-K_σ for open mode and K_τ for shear mode) are worked out with Eq. 1:

$$K_\sigma = \frac{\cos\theta}{2}\left[\frac{K_I\cos^2\theta}{2} - \frac{3}{2}K_{II}\sin\theta\right] \quad (1a)$$

$$K_\tau = \frac{1}{2}\cos\theta \frac{}{2}[K_I\sin\theta - K_{II}(3\cos\theta - 1)] \quad (1b)$$

When $K_{\sigma max} > K_{\sigma th}$, the crack will propagate in mode 1 and the propagation direction will be at the angle of θ_σ (where $K_{\sigma max} = K_\sigma(\theta_\sigma)$), where $\Delta K_{\sigma th}$ is the fracture threshold of SIF of Mode I. Also, when $K_{\tau max} > K_{\tau th}$, the crack will propagate in Mode II and the propagation direction will be at the angle of θ_τ (where $K_{\tau max} = K_\tau(\theta_\tau)$), where $\Delta K_{\tau th}$ is the fracture threshold of SIF of mode 2. According to the research of Otsuka *et al.* (1975), the fracture thresholds of SIF of low carbon steel are $K_{\sigma th} \approx 6$, $K_{\tau th} \approx 1.5$ Mpa $m^{1/2}$. In this study, the crack propagation criterion and propagation direction calculation will follow Kaneta and Murakami's research. Crack Propagation Rate under RCF.

Under the act of complicated RCF, the propagation of the rail crack can't be simply predicted with Paris equation (Erdogan and Sih, 1963). The joint action of mode 1 and 2 loadings should be taken into account at the same time. The Paris equation can be rewritten in Eq. 2 as:

$$\frac{da}{dN} = C(\Delta K_V)^n \quad (2)$$

Or in logarithm form in Eq. 3:

$$\ln\frac{da}{dN} = \ln C + \ln(\Delta K_V)^n = \ln C + n.\ln\Delta K_V \quad (3)$$

ΔK_V is the corrective value of SIF range which has taken into account the joint action of mode 1 and 2 loadings, C and n are material coefficients which indicate the inherent fracture mechanics properties of certain material and usually got through experiments.

Under the act of RCF, the magnitude of K_{III} during the propagation of rail crack is relatively small compared with K_I and K_{II} which can be neglected. Then ΔK_V can be calculated with Eq. 4:

$$\Delta K_V = \sqrt{\Delta K_I^2 + \Delta K_{II}^2} \quad (4)$$

Schnitzer (2007) conducted similar derivation based on Richard's research and rewrote the SIF range at crack tip during its stable propagation under the complex loads. According to Schnitzer (2007), correcting the SIF range with energy releasing rate is better which is expressed in Eq. 5, namely:

$$\sqrt{\text{^0\_D\_D}} \quad (5)$$

In this study, the analysis of the rail crack propagation can be assumed as coplanar crack, so Eq. 5 is used to correct the SIF range.

According to Schnitzer's fracture test of UIC60 rail sample, the values of material coefficients C and n can be concluded with its deformation and listed in Table 1. The crack propagation rate can be calculated with Eq. 2 or 3 together with Eq. 5 and the data listed in Table 1.

3D finite element model: This study is mainly subjected to the study of the propagation of multiple rail cracks under RCF, especially the effect of the crack size, so a 3D FE model is established in ABAQUS to simulation the RCF between rail and wheel. The basic idea of building the model is expressed in Fig. 1. It is assumed that there are two half-circular cracks on the rail surface, the central line of each crack coincide with the longitudinal axis of the rail, namely the z axis. The radii of the two cracks are α_1 and α_2 and the angles between the rail surface and the crack surfaces are α_1 and α_2. Since, the most head checks are parallel to each other, so $\alpha_1 = \alpha_2 = \alpha$.

The geometric model is established according to the profiles of UIC 60 rail and S1002 wheel to stimulate the actual RCF between rail and wheel. Two crack models are inserted into the FE geometric model with Zencrack software and 33 notes are defined along the crack front (Fig. 2). The calculation of SIF K_I and K_{II} at each note along the crack front is conducted by ABAQUS as the

Table 1: Statistical value of C and n of UIC 60 Rail

Depth of crack (mm)	Deformation (%)	No.	LgC	C(Mpa$\sqrt{m}$)$^{-n}$.mn
0		1.902	-9.130	7.4214E-10
1.45	33.10	2.252	-10.37	4.2636E-11
2.15	20.50	2.419	-10.96	1.0916E-11
2.95	10.70	2.933	-12.40	3.9738E-13
5	0.00	5.477	-19.70	1.9828E-20

wheel passes the surface crack of the rail and the results at point C_1 and point $A_1(B_1)$ of the old crack are discussed in the study.

The FE model is applied to simulate the situation that near to the old rail crack initiates a new crack and mainly focus on the effect of the new crack size during the old crack propagation, so the distance between the two cracks is assumed as a constant as well as the radius of the old crack. By varying the parameters listed in Table 2, several simulations are carried out to calculate the FIS at the crack tips.

In Table 2, α_1 is the radius of the old crack and α_2 is the radius of the new one. t is used to define the distance between the two cracks, when t >0, it means the wheel will pass the old crack first then the new crack; when t<0, it means the wheel will pass the new crack first. F_N is the axle load on each wheel, f is the coefficient of friction between rail and wheel and fc is the coefficient of friction between crack surfaces, α -D-Dd-ÿá- D-Dd-ÿá-Dd-á-D-Dd-Ø-Ĉ-+-Ĉ-*-Ĉ-*-Ĉ-*-Ĉ-j*-Ĉ-Ċ.

Table 2: Parameters of FE model

α (mm)	t (mm)	F_N (N)	f	f_c	α (°)
$\alpha_1 = 5$	-10	100000	+0.1	0.2	30
$\alpha_2 = 3$	+10				
$\alpha_1 = 5$	-10	100000	+0.1	0.2	30
$\alpha_2 = 5$	+10				
$\alpha_1 = 5$	-10	100000	0.1	0.2	30
$\alpha_2 = 7$	+10				

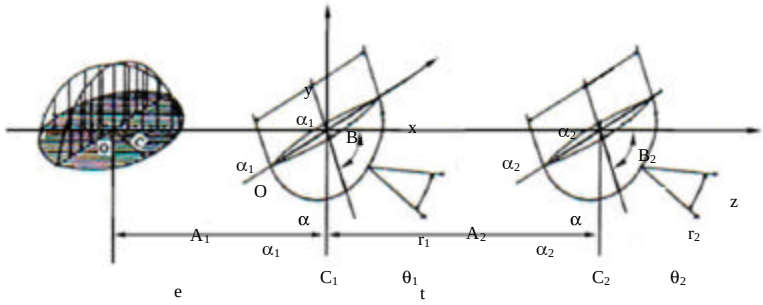

Fig. 1: Coordinate system of multiple rail crack model

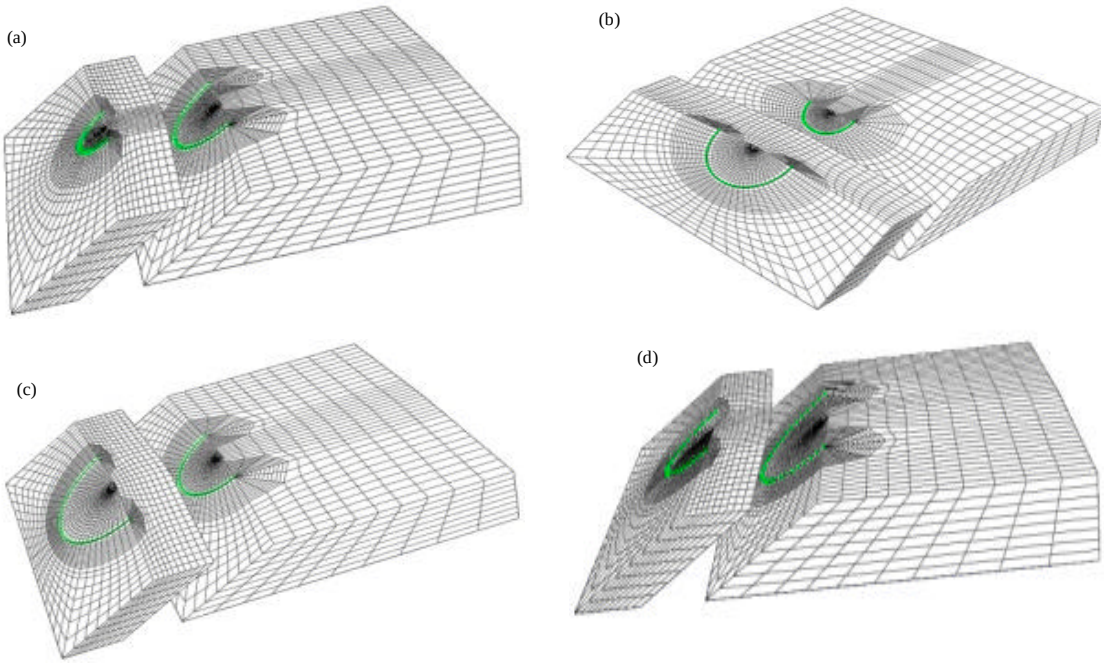

Fig. 2(a-d): Meshes of 3D rail FE models with multiple cracks (a) α_1 = 5 mm, α_2 = 3 mm, (b) α_1 = 5 mm, α_2 = 3 mm, (c) α_1 = 5 mm, α_2 = 7 mm and (d) α_1 = 5 mm, α_2 = 7mm

RESULTS AND DISCUSSION

From Fig. 3 and 4, it is clear to see with the initiation of a new crack near to the old rail crack, the stress level at point C_1, the deepest point at the old crack front, is lower compared with single crack situation. And with the increase of the new crack size, the stress intensity at point C_1 is decreased. The stress at point A_1 and B_1 at the rail surface is also redistributed, just the same as point C_1, where the stress intensity is smaller than no neighboring crack and it is decreased as the neighboring crack size increases.

The location of the new crack also has an effect on the stress distribution at the old crack tips. The SIFs of the crack tips on the old crack will be reduced more when the contact load is applied on the new crack.

With the SIFs calculated with the FE model, whether crack will propagate at point C_1 and point $A_1(B_1)$ can be determined according to Kaneta and Murakami's method and the propagation direction can be predicted with Eq. 1. Also the crack propagation rate can be calculated with Eq. 2 or 3 together with Eq. 5 and the parameters listed in Table 1. The propagation of point C_1 and point $A_1(B_1)$ is listed in Table 3-6, where a is the size of the crack, θ_0 is

Table 3: Crack propagation at point C1 when t = -10 mm

α (mm)	Whether propagate	Propagation mode	Propagation angle θ_0 (°)	K_{max}(MPa(m)$^{1/2}$)	$\frac{da}{dN}$ (10^{-8} mm)
$\alpha_1 = 5$ $\alpha_2 = 0$	Yes	II	0.0002	24	3.3127
$\alpha_1 = 5$ $\alpha_2 = 3$	Yes	II	0.0002	21.74	2.8377
$\alpha_1 = 5$ $\alpha_2 = 5$	Yes	II	0.0002	21.07	2.4797
$\alpha_1 = 5$ $\alpha_2 = 7$	Yes	II	0.0002	19.66	1.9914

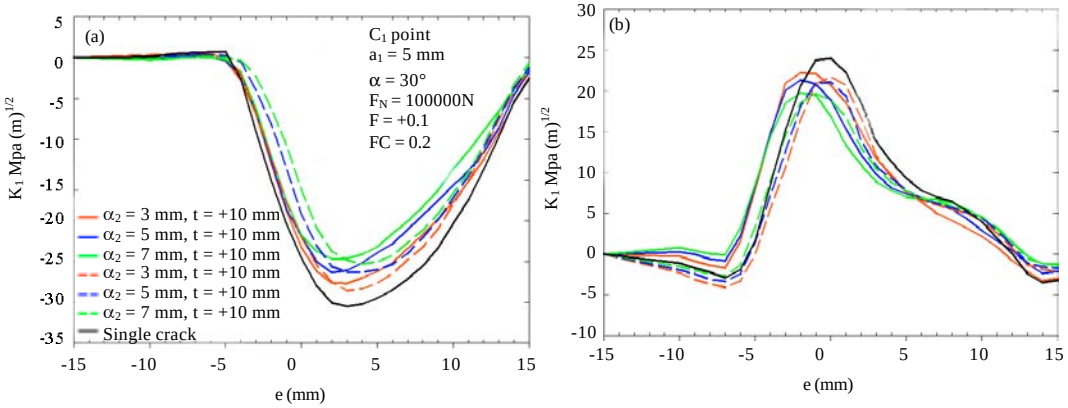

Fig. 3(a-b): SIF at point C_1 of the crack tip with different neighboring crack sizes (a) K_I and (b) K_{II}

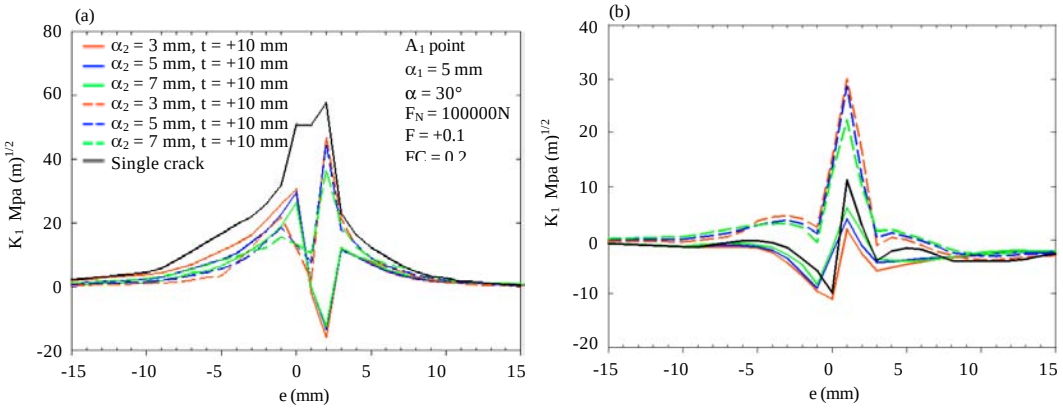

Fig. 4(a-b): SIF at point $A_1(B_1)$ of the crack tip with different neighboring crack sizes (a) K_I and (b) K_{II}

Table 4: Crack propagation at point C1 when t = +10 mm

α (mm)	Whether propagate	Propagation mode	Propagation angle θ_0 (°)	K_{max} (Mpa(m)$^{1/2}$)	$\frac{da}{dN}$ (10^{-8} mm)
$\alpha_1 = 5$ $\alpha_2 = 0$	Yes	II	0.0002	24.00	3.3127
$\alpha_1 = 5$ $\alpha_2 = 3$	Yes	II	0.0002	22.23	2.7536
$\alpha_1 = 5$ $\alpha_2 = 5$	Yes	II	0.0002	21.36	2.3129
$\alpha_1 = 5$ $\alpha_2 = 7$	Yes	II	0.0002	19.79	1.7259

Table 5: Crack propagation at point $A_1(B_1)$ when t = -10 mm

α (mm)	Whether propagate	Propagation mode	Propagation angle θ_0 (°)	K_{max} (Mpa (m)$^{1/2}$)	$\frac{da}{dN}$ (10^{-5} mm)
$\alpha_1 = 5$ $\alpha_2 = 0$	Yes	I	-3.38	58.54	0.1838
$\alpha_1 = 5$ $\alpha_2 = 3$	Yes	I	-32.68	54.69	0.1791
$\alpha_1 = 5$ $\alpha_2 = 5$	Yes	I	-26.34	49.10	0.1569
$\alpha_1 = 5$ $\alpha_2 = 7$	Yes	I	-25.60	42.19	0.0986

Table 6: Crack propagation at point A1(B1) when t = +10 mm

α (mm)	Whether propagate	Propagation mode	Propagation angle θ_0 (°)	K_{max} (Mpa(m)$^{1/2}$)	$\frac{da}{dN}$ (10^{-5} mm)
$\alpha_1 = 5$ $\alpha_2 = 0$	Yes	I	-3.38	58.54	0.1838
$\alpha_1 = 5$ $\alpha_2 = 3$	Yes	I	33.01	35.59	0.0582
$\alpha_1 = 5$ $\alpha_2 = 5$	Yes	I	9.12	29.87	0.0548
$\alpha_1 = 5$ $\alpha_2 = 7$	Yes	I	6.17	26.52	0.0481

the propagation angle which defines the propagation direction of the crack, K_{max} is the maximum stress intensity factor which causes the crack to propagation and da/dN is the propagation rate. t defines the distance between the two cracks which has been mentioned in the FE model part.

From the results shown in Table 3 and 4, it is clear that for the deepest point C_1 at the crack tip front, the crack propagation direction will keep the same either the new crack initiates in front of the old crack or behind it in the traction direction, the propagation angle is the same as there is no neighboring crack around. The crack propagation rate at point C_1 is decreased as the neighboring crack size increases. For the same neighboring crack size, the crack propagation rate is higher when the wheel passes the new crack first and then the old crack.

From the results shown in Table 5 and 6, It can also be seen that for the surface point $A_1(B_1)$ at the crack tip front, the crack propagation direction will change, the propagation angle is decreased and bends to the neighboring crack. The crack propagation rate at point A_1 is also decreased as the neighboring crack size increases. For the same neighboring crack size, the crack propagation rate is higher when the wheel passes the new crack first and then the old crack.

CONCLUSION

In this study, the propagation of multiple rail surface cracks is simulated in ABAQUS with a 3D model. The SIFs at the deepest point (C_1) and rail surface point (A_1 and B_1) at the crack tip front with a neighboring crack are calculated and discussed. The propagation direction and propagation rates at these points are also predicted according to Kaneta and Murakami's research as well as Schnitzer's tests.

From the simulation results, it can be concluded that when there is a new rail crack initiating near to the old rail crack with the distance of 10 mm which is the approximate size of the contact diameter, the propagation rate of the old crack will be decreased as the new crack increases. The propagation direction at point C_1 will not change and the old crack will propagate in the same direction as there is no neighboring crack. While the propagation direction of point A_1 and B_1 will bend to the new crack which may result in the joint of these two cracks to form either spalling or a new crack propagating downward and cause final rail fracture. As the distance between these two rail surface cracks changes, the stress distribution at the rail and the crack tips will change also. When they are far enough, the neighboring crack will have no influence on the propagation of the old rail crack. The effect of the

crack distances on the propagation trend of multiple rail surface cracks under RCF will be discussed in another study.

ACKNOWLEGMENT

This study is supported by Science and Technology Program of Shanghai Maritime University (20110037) as well as Shanghai Municipal Education Commission Special Research Fund for Excellent Young College and University Teachers 2010.

REFERENCES

Benuzzi, D., E. Bormetti and G. Donzella, 2003. Stress intensity factor range and propagation mode of surface cracks under rolling-sliding contact. Theoretical Applied Fracture Mechanics, 40: 55-74.

Brouzoulis, J. and M. Ekh, 2012. Crack propagation in rails under rolling contact fatigue loading conditions based on material forces. Int. J. Fatigue, 45: 98-105.

Canadinc, D., H. Sehitoglu and K. Verzal, 2008. Analysis of surface crack growth under rolling contact fatigue. Int. J. Fatigue, 30: 1678-1689.

Cookson, J.M. and P.J. Mutton, 2011. The role of the environment in the rolling contact fatigue crack of rails. Wear, 271: 113-119.

Donzella, G., M. Faccoli, A. Ghidini, A. Mazzu and R. Roberti, 2005. The competitive role of wear and RCF in a rail steel. Eng. Fracture Mechanics, 72: 287-308.

Dubourg, M.C. and V. Lamacg, 2002. A predictive rolling contact fatigue crack growth model: Onset of branching direction and growth-role of dry and lubricated conditions on crack patterns. J. Tribol., 124: 680-688.

Erdogan, F. and G. Sih, 1963. On the crack extension in plates under plane loading and transverse shear. J. Basic Eng., 85: 519-525.

Fajdiga, G., Z. Ren and J. Kramar, 2007. Comparison of virtual crack extension and strain energy density methods applied to contact surface crack growth. Eng. Fracture Mechanics, 74: 2721-2734.

Fletcher, D.I., L. Smith and A. Kapoor, 2009. Rail rolling contact fatigue dependence on friction, predicted using fracture mechanics with a three-dimensional boundary element model. Eng. Fracture Mechanics, 76: 2612-2625.

Hearle, A.D. and K.L. Johnson, 1987. Cumulative plastic flow in rolling and sliding line contact. J. Applied Mechanics, 54: 1-7.

Jiang, Y., B. Xu and H. Sehitoglu, 2002. Three-dimensional elastic-plastic stress analysis of rolling contact. J. Tribol., 124: 699-708.

Kaneta, M., M. Suetsugu and Y. Murakami, 1986. Mechanism of surface crack growth in lubricated rolling/sliding spherical contact. J. Applied Mechanics, 53: 354-360.

Keer, L.M., M.D. Bryant and G.K. Haritos, 1982. Subsurface and surface cracking due to Hertzian contact. J. Lubrication Technol., 104: 347-351.

Lewis, R. and U. Olsson, 2009. Wheel-Rail Interface Handbook. CRC Press, USA., ISBN: 9781439801468, Pages: 842.

Makino, T., T. Kato and K. Hirakawa, 2012. The effect of slip ratio on the rolling contact fatigue property of railway wheel steel. Int. J. Fatigue, 36: 68-79.

Muster, H., H. Schmedders, K. Wick and H. Pradier, 1996. Rail rolling contact fatigue. The performance of naturally hard and head-hardened rails in track. Wear, 191: 54-64.

Otsuka, A., K. Mori and T. Miyata, 1975. The condition of fatigue crack growth in mixed mode condition. Eng. Fracture Mechanics, 7: 429-432.

Ringsberg, J.W., 2005. Shear mode growth of short surface-breaking RCF cracks. Wear, 258: 955-963.

Schnitzer, T., 2007. Bruchmechanische analyse des wachstums von rollkontaktermudungsrissen in eisenbahnschienen. [Fracture mechanics analysis of the growth of rolling contact fatigue cracks in railroad tracks]. Ph.D. Thesis, Berlin Technische Universitaet, Berlin, Germany.

Seo, J.W., S.J. Kwon, H.K. Jun and D.H. Lee, 2011. Numerical stress analysis and rolling contact fatigue of white etching layer on rail steel. Int. J. Fatigue, 33: 203-211.